VOL. 7, NO. 7, JULY 2012 ISSN 1819-6608
ARPN Journal of Engineering and Applied Sciences

www.arpnjournals.com

A HYBRID CASCADED SEVEN - LEVEL INVERTER WITH MULTICARRIER MODULATION TECHNIQUE FOR FUEL CELL APPLICATIONS

T. Thamizhselvan[1] and R. Seyezhai[2]
[1]Department of Electrical and Electronics Engineering, Rajalakshmi Engineering College, Chennai, Tamil Nadu, India
[2]Department of Electrical and Electronics Engineering, SSN College of Engineering, Chennai, Tamil Nadu, India
E-Mail: tamilselvan84@gmail.com

ABSTRACT

This paper proposes a single-phase seven -level hybrid cascaded multilevel inverter (HCMLI) for fuel cell system, with a novel Pulse Width Modulation (PWM) technique. The proposed modulation technique employs multi carrier waveforms and a single reference sine wave was used to generate the PWM signals. A two phase Interleaved Boost Converter (IBC) between the Proton Exchange Membrane Fuel Cell (PEMFC) and the HCMLI is introduced to reduce the input current ripples and also to convert low voltage high current input into a high voltage low current output. The inverter circuit topology has been described in detail and their performance has been verified based on Total Harmonic Distortion using MATLAB/SIMULINK.

Keywords: proton exchange membrane fuel cell, hybrid cascaded multilevel inverter, interleaved boost converter, total harmonic distortion.

1. INTRODUCTION

A distributed energy source consisting of a fuel cell normally requires a high power boost converter for energy management to assist the slow responding fuel cell. Comparison with the other types of fuel cells, Proton Exchange Membrane (PEM) fuel cell shows charming attraction with its advantages such as low temperature, high power density, fast response and zero emission. In this paper, a two phase Interleaved Boost Converter (IBC) between the Proton Exchange Membrane Fuel Cell (PEMFC) and the hybrid multilevel inverter (HCMLI) has been introduced to reduce the input current ripples and also the steady-state voltage ripples at the output capacitors of IBC are reduced.

There are several types of multilevel inverters has been proposed but the one Considered in this work is the hybrid cascade multilevel inverter. In this paper, a seven-level HCMLI is used instead of conventional three-level inverter because it offer grater advantages, such as improved output waveform, smaller filter size, lower EMI and lower THD. The new inverter topology offers an important improvement in terms of less component count and reduced complexity when compared with the other conventional inverters [1]. A seven-level HCMLI topology [2-3] is interfaced with PEMFC via 2-phase interleaved boost converter, as shown in Figure-1. An auxiliary circuit comprising for diodes and a switch is configured together with a conventional full-bridge inverter to form this topology.

A novel PWM modulation technique is used to generate switching signals for the switches and to generate seven output-voltage levels: 0, +Vdc/3, +2Vdc/3, +Vdc, -Vdc/3, -2Vdc/3,-Vdc. Simulation results are presented to validate the proposed inverter configuration.

2. HYBRID SEVEN-LEVEL INVERTER

The proposed single-phase seven-level inverter consist of single-phase conventional H-bridge inverter, two bidirectional switches and a capacitor voltage divider formed by C_1, C_2, and C_3, as shown in Figure-1. The modified H-bridge topology is significantly advantageous over other topologies, i.e., less power switch, power diodes, and less capacitor for inverters of the same number of levels. Proper switching of the inverter can produce seven output-voltage levels (0, $+V_{dc/3}$, $+2V_{dc/3}$, $+V_{dc}$, $-V_{dc/3}$, $-2V_{dc/3}$, $-V_{dc}$). The proposed inverter operation can be divided into seven switching states, as shown in the Table-1.

a. **To obtain + V_{dc}:** S_1 is ON and S_4 is ON. All other controlled switches are OFF, the voltage applied to the load terminals is + V_{dc}.

b. **To obtain + $2V_{dc}/3$:** The bidirectional switch S_5 is ON and S_4 is ON. All other controlled switches are OFF, the voltage applied to the load terminals is + $2V_{dc}/3$.

c. **To obtain + $V_{dc}/3$:** The bidirectional switch S_6 is ON and S_4 is ON. All other controlled switches are OFF, the voltage applied to the load terminals is + $V_{dc}/3$.

ARPN Journal of Engineering and Applied Sciences

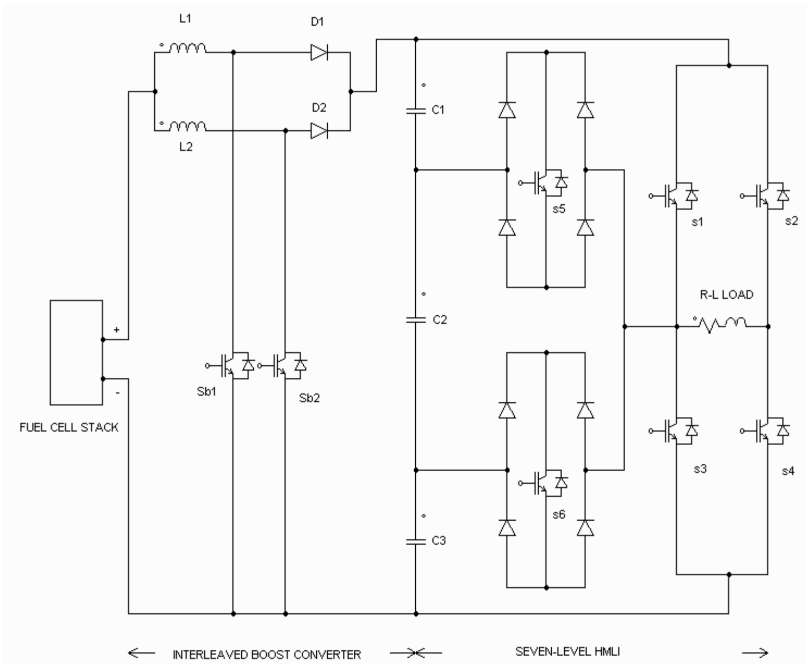

Figure-1. Hybrid cascaded multilevel inverter for fuel cell system.

d) **To obtain Zero output:** This level can be produced by two switching combinations; switches S_3 and S_4 are ON, or $S_1$and S_2 are ON, and all other controlled switches are OFF, the voltage applied to the load terminals are zero.

e) **To obtain - V_{dc} /3:** The bidirectional switch S_5 is ON and S_2 is ON. All other controlled switches are OFF, the voltage applied to the load terminals is - V_{dc} /3.

f) **To obtain -2V_{dc}/3:** The bidirectional switch S_6 is ON and S_2 is ON. All other controlled switches are OFF, the voltage applied to the load terminals is - 2V_{dc} /3.

g) **To obtain - V_{dc}:** S_2 is ON and S_3 is ON. All other controlled switches are OFF, the voltage applied to the load terminals is - V_{dc}.

Table-1. Conduction table for HCMLI.

Vo	S1	S2	S3	S4	S5	S6
Vdc	On	Off	Off	On	Off	Off
2 Vdc/3	Off	Off	Off	On	On	Off
Vdc/3	Off	Off	Off	On	Off	On
0	On	On	On	On	Off	Off
-Vdc	Off	On	Off	Off	On	Off
-2 Vdc/3	Off	On	Off	Off	Off	On
-Vdc/3	Off	On	On	Off	Off	Off

3. MODULATION STRATERGY FOR HYBRID MULTILEVEL INVERTER

In this paper single reference signal is compared with multiple carrier signals to generate PWM signal. A novel modulation technique [4-6] was proposed to generate PWM signals. Multiple carrier signals were compared with single sine reference signal, the carrier signals had the same frequency and amplitude. The carrier signals were each compared with the reference signal to generate the switching pattern. If $V_{carrier1}$ had exceeded the amplitude of Vref, $V_{carrier2}$ was compared with Vref until it had exceeded the amplitude of Vref Then, onward, $V_{carrier3}$ would be compared with Vref until Vref reached zero. Once $V_{carrier3}$ exceeded the amplitude of Vref, $V_{carrier2}$ was compared with Vref until it had exceeded the amplitude of Vref. Then, onward, $V_{carrier3}$ would be compared with Vref until Vref reached zero. Figure-2 shows the resulting switching pattern. Switches S_1, S_3, S_5, and S_6 would be operated at the rate of the carrier signal frequency, whereas S_2 and S_4 would operate at the rate of reference frequency.

Modulation index ma for seven-level inverter is given as [2]:

$$m_a = \frac{A_m}{3A_c} \quad (1)$$

where A_c is the peak-to-peak value of carrier and A_m is the peak value of voltage reference Vref.

4. INTERLEAVED BOOST CONVERTER

Interleaved Boost Converter (IBC) topologies have received increasing attention in recent years for high power applications. It serves as a suitable interface for fuel

VOL. 7, NO. 7, JULY 2012 ISSN 1819-6608
ARPN Journal of Engineering and Applied Sciences

cells to convert low voltage high current input into a high voltage low current output.

The advantages of interleaved boost converter compared to the classical boost converter are low input current ripple, high efficiency, faster transient response, reduced electromagnetic emission and improved reliability. Higher efficiency is realized by splitting the output current into 'n' paths, substantially reducing I^2R losses and inductor losses. The gating pulses of the switches of the two phases are shifted by 360/n, i.e., 360/2 for n = 2, which is 180 degrees and it is shown in Figure-3.

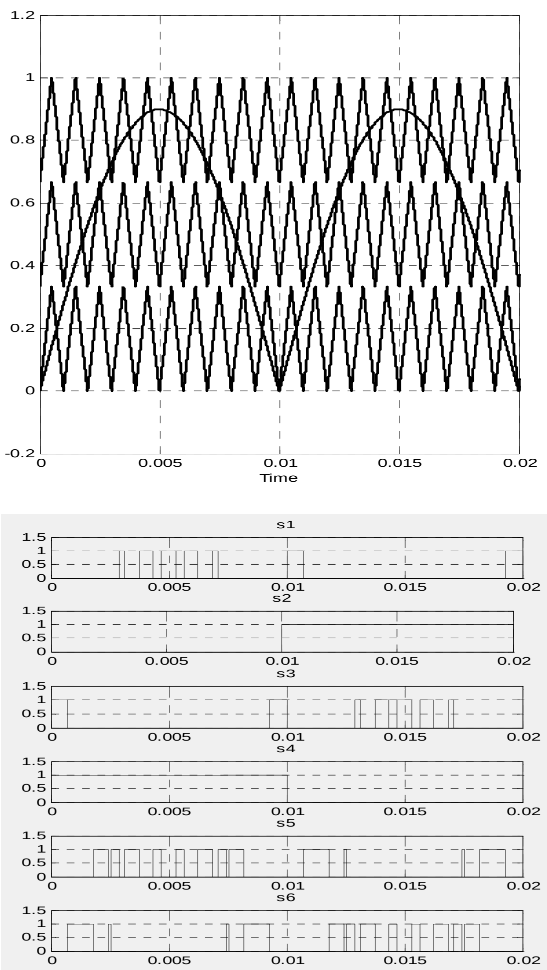

Figure-2. Multiple carrier PWM technique and switching pattern for HCMLI.

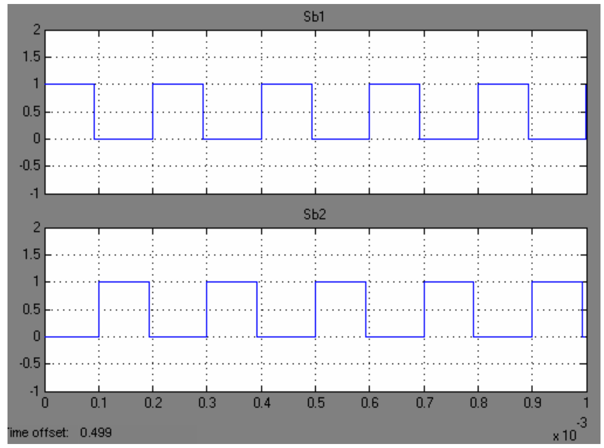

Figure-3. Switching pattern for 2-phase IBC

5. DESIGN CONSIDERATIONS OF IBC

The interleaved boost converter design [8-9] involves the selection of the number of phases, the inductors, the output capacitor and the power switches. Both the inductors and diodes should be identical in all the channels of an interleaved design. In order to select these components, it is necessary to know the duty cycle range and peak currents. Since the output power is channeled through 'n' power paths where 'n' is the number of phases, a good starting point is to design the power path components using 1/n times the output power. Basically, the design starts with a single boost converter operating at 1/n times the power.

5.1 Choosing the number of phases

This paper utilizes two phases since the ripple content reduces with increase in the number of phases. The ripple reduces to 12% of that of a conventional boost converter. If the number of the phases is increased further, without much decrease in the ripple content, the complexity of the circuit increases very much, thereby increasing the cost of implementation. Hence, as a tradeoff between the ripple content and the cost and complexity, number of phases is chosen as two. The number of inductors, switches and diodes are same as the number of phases and switching frequency is same for all the phases [10].

5.2 Selection of duty ratio

The decision of the duty cycle is based on the number of phases. This is because depending upon the number of phases; the ripple is minimum at a certain duty ratio [10]. For two phase interleaved boost converter, the ripple is minimum at duty ratio, D = 0.45. Hence, the design value of the duty ration is chosen as 0.45.

5.3 Selection of capacitance and inductance

The selection of capacitance and inductance is done using the formulae.

$$C = VoDF/R\Delta Vo \quad (2)$$

ARPN Journal of Engineering and Applied Sciences

www.arpnjournals.com

where Vo represents the output voltage (V), D represents the duty ratio, F represents frequency (Hz), R represents resistance (Ω) and ΔVo represents the change in the output voltage (V).

$$L = VsD/\Delta i_L F \quad (3)$$

where Vs represents the source voltage and i_L represents the inductor current ripple.

5.4 Selection of power devices

Power diodes are used for lower cut-in voltage, higher reverse leakage current, higher operating frequency. IGBT is used as a switching device since it is a voltage controlled device, having high input impedance. With rise in temperature, the increase in on-state resistance in IGBT is not much pronounced; so on-state voltage drop and losses do not rise rapidly.

6. MODELING OF FUEL CELL

Proton Exchange Membrane Fuel Cell (PEMFC) combines hydrogen and oxygen over a platinum catalyst to produce electrochemical energy with water as the byproduct. Figure-4 shows the V-I characteristics of a typical single cell operating at room temperature and normal air pressure. The variation of the individual cell voltage is found from the maximum cell voltage and the various voltages drops (losses). The output voltage of a single cell can be defined as:

$$V_{fc} = E_{nernst} - V_{act} - V_{ohm} - V_{conc} \quad (4)$$

Where E_{nerst} represents the reversible voltage; V_{act} is the voltage drop due to the activation of the anode and cathode; V_{ohm} is a measure of ohmic voltage drop associated with the conduction of the protons through the solid electrolyte and electrons through the internal electronic resistances; V_{conc} represents the voltage drop resulting from the concentration or mass transportation of the reacting gases. E_{nerst} represent the no-load voltage, while the sum of all the other terms gives the reduction of the useful voltage achievable at the cell terminals, when a certain load current is required. For n cells connected in series and forming a stack, the voltage (E_{cell}), can be calculated by:

$$E_{cell} = n * V_{fc} \quad (5)$$

Several factors are responsible for the voltage drop in a fuel cell [11-12] and they are referred as polarization. The losses originate from three sources namely activation polarization, ohmic polarization and concentration polarization.

6.1 Activation polarization

The activation over voltage is the voltage drop due to the activation of anode and cathode. It can be calculated as:

$$V_{act} = -[\varepsilon_1 + \varepsilon_2 * T + \varepsilon_3 * T * \ln(C_{o2}) + \varepsilon_4 * \ln(I_{stack})] \quad (6)$$

where, I_{stack} is the cell operating current (A), and the ε_i's represent parametric coefficients for each cell model, whose values are defined based on theoretical equations with kinetic, thermodynamic, and electrochemical foundations. C_{o2} is the concentration of oxygen.

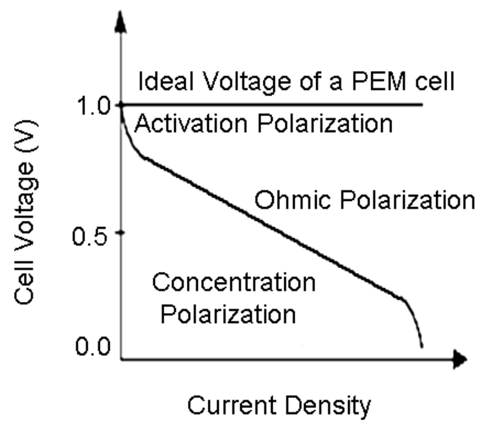

Figure-4. Ideal V-I characteristics of a single PEMFC.

6.2 Ohmic polarization

This loss occurs due to the electrical resistance of the electrodes and the resistance to the flow of ions in the electrolyte. It is given by:

$$V_{ohm} = I_{stack} * (R_m + R_C) \quad (7)$$

where R_c represents the resistance to the transfer of protons through the membrane, usually considered constant and R_m is:

$$R_m = \rho_m * \frac{l}{A} \quad (8)$$

Where ρ_m is the specific resistivity of the membrane for the electron flow (cm), A is the cell active area cm and l is the thickness of the membrane (cm), which serves as the electrolyte of the cell.

6.3 Concentaration polarization

This is due to the change in concentration of reactants at the surface of the electrodes as the fuel is used causing reduction in the partial pressure of reactants, resulting in reduction in voltage given by:

$$V_{conc} = -\frac{RT}{n} * F * ln\left[l - \frac{i}{i_1}\right] \quad (9)$$

In this paper, dynamic model of a PEM fuel cell [13-14] system developed in MATLAB-SIMULINK is presented. A PEM fuel cell system is designed using fuel cell stack. A PEM fuel cell which has values of 6 kW, 45 V DC is used. Maximum power of the fuel cell stack

ISSN 1819-6608
ARPN Journal of Engineering and Applied Sciences

reaches to 8.325 kW by adjusting the fuel flow rate 85 lpm). Table-2 shows the PEMFC specifications.

Table-2. Fuel cell specifications.

No. of cells	45V
R	0.0756 ohms
P_{H2}	1.5 bar
P_{O2}	1 bar
Fuel cell temp.	338 kelvin
Flow rate of H_2	50.06pm

7. SIMULATION RESULTS

To obtain the V-I characteristics of the PEM fuel cell, the model is simulated using MATLAB/SIMULINK for the following values of input variables: P_{H2} (anode pressure) = 1.5 bar, P_{O2} (cathode pressure) = 1bar, T (temperature of the cell) = 323K. The simulated V-I characteristics of a single PEM fuel cell are shown in Figure-5 which depicts the various polarization losses.

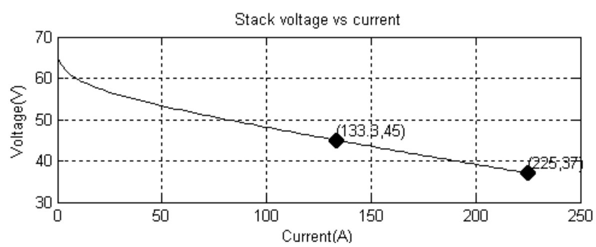

Figure-5. V-I characteristics of PEMFC.

The work presents the proposed multiple carrier PWM technique for the hybrid seven-level cascaded multilevel inverter is simulated using MATLAB-SIMULINK with the parameters shown in Table-3. The investigation is made in terms of THD.

Table-3. Simulation parameters.

Output fuel cell voltage V_{fc}	**45 V**
Output boost converter voltage V_o	100 V
Output load voltage V_l	100 V
Switching frequency F_s	10KHz
R	10 ohms
L	3.3mH

The input current ripple, and output voltage ripple obtained from PEMFC connected to interleaved boost converter are shown in Figure-6 and Figure-7.

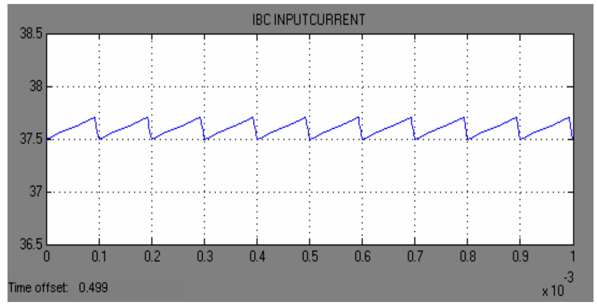

Figure-6. Input current ripple of 2-phase IBC.

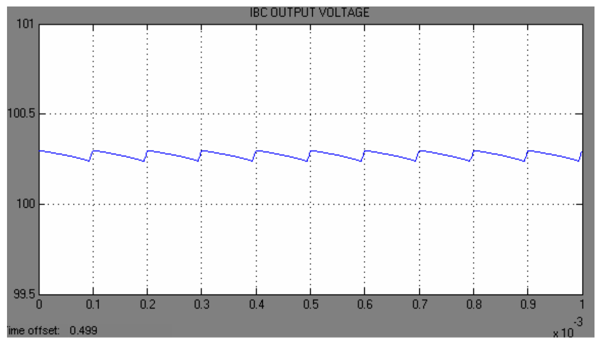

Figure-7. Output voltage ripple of 2-phase IBC.

The input current ripple and output voltage ripple for a boost converter interfaced with the fuel cell are shown in Figures 8 and 9.

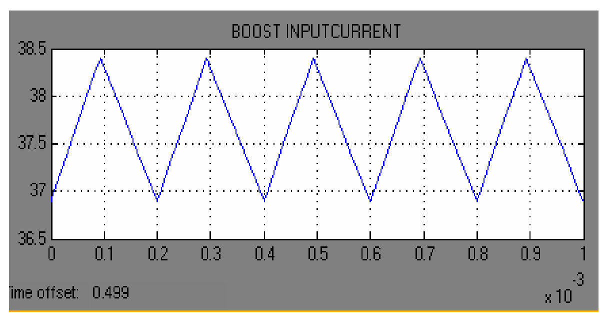

Figure-8. Input current ripple of boost converter.

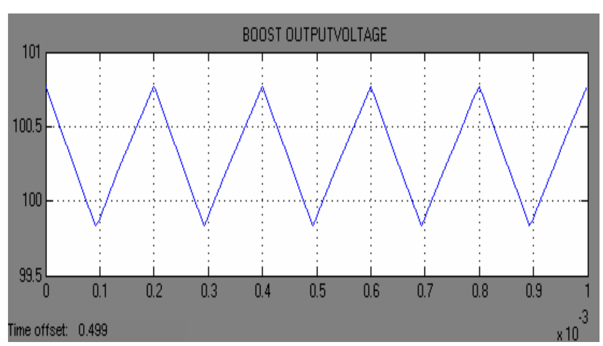

Figure-9. Output voltage ripple of boost converter.

ARPN Journal of Engineering and Applied Sciences

www.arpnjournals.com

The simulation results of IBC are compared to that of a PEMFC connected to a boost converter which is shown in Table-4.

Table-4. Comparison of IBC and boost converter.

Parameter	Boost converter	IBC
Input current ripple	1.76%	0.08%
Output voltage ripple	13.8%	7.36%
Inductor current ripple	0.87%	0.04%

The work presents the proposed multiple carrier PWM technique for the hybrid seven-level cascaded multilevel inverter is simulated using MATLAB-SIMULINK with the parameters shown in Table-3. The investigation is made in terms of THD.

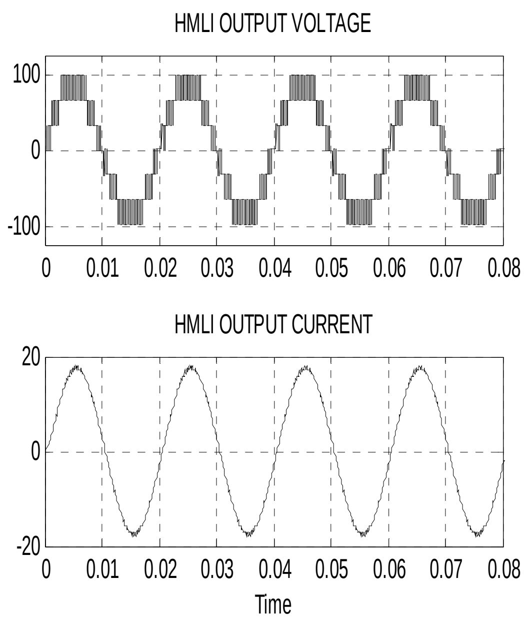

Figure-10. Output voltage and current waveforms for HCMLI.

The output voltage and current waveforms for HCMLI interfaced with the fuel via IBC are shown in Figure-10. Figure-11 shows the THD measurements, the seven-level HCMLI produced the lowest THD compared with the five and three-level inverter. This proves that, as the level increases, the THD reduces.

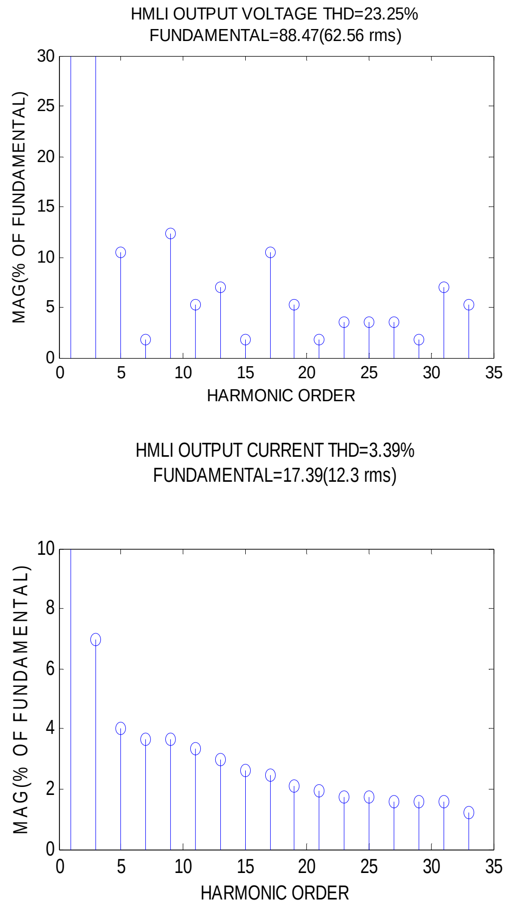

Figure-11. THD results of output voltage and current waveforms for HCMLI.

CONCLUSIONS

The proposed seven-level HCMLI with reduced number of switches gives a reduced THD compared to the conventional MLI. A two phase Interleaved Boost Converter between the Proton Exchange Membrane Fuel Cell and the HCMLI has been designed and analyzed. It is found that IBC effectively reduces the overall current ripple compared to that of boost converter. Also this paper presented a novel PWM switching scheme for the proposed multilevel inverter. It utilizes multiple carrier signals and a sine reference signal to generate PWM switching signals. Therefore, HCMLI with multiple carrier PWM technique is a suitable topology for fuel cell applications.

REFERENCES

[1] J. Rodriguez, J. S. Lai, and F. Z. Peng. 2002. Multilevel inverters: A survey of topologies, controls, and applications. IEEE Trans. Ind. Electron. 49(4): 724-738.

[2] N. A. Rahim and J. Selvaraj. 2010. Multi-string five-level inverter with novel PWM control scheme for PV

application. IEEE Trans. Ind. Electron. 57(6): 2111-2121.

[3] G. Ceglia, V. Guzman, C. Sanchez, F. Ibanez, J. Walter and M. I. Gimanez. 2006. A new simplified multilevel inverter topology for DC-AC conversion. IEEE Trans. Power Electron. 21(5): 1311-1319.

[4] M. Calais and V. G. Agelidis. 1998. Multilevel converters for single-phase grid connected photovoltaic systems-An overview. In: Proc. IEEE Int. Symp.Ind. Electron. 1: 224-229.

[5] V. G. Agelidis, D. M. Baker, W. B. Lawrance and C. V. Nayar. 1997. A multilevel PWMinverter topology for photovoltaic applications. In: Proc. IEEE ISIE, Guimäes, Portugal. pp. 589-594.

[6] Martha Calais, Lawrence J. Borlel Vassilios and G. Agelidis. 2001. Analysis of Multicarrier PWM Methods for a Single-phase Five Level Inverter. IEEE Transactions on Power Electronics. pp. 1351-1356.

[7] McGrath B.P and Holmes D.G. 2002. Multicarrier PWM strategies for Multilevel Inverters. IEEE Transactions on Industrial Electronics. 49(4): 858-867.

[8] Choe G.Y., Kang H.S., Lee B.K. and Lee W.L. 2007. Design consideration of Interleaved Converters for fuel cell applications. In: Proc. International conference on Electrical machines and Systems, Seoul. pp. 238-243.

[9] Shin H.B., Park J.G., Chung S.K., Lee. H.W. and Lipo T.A. 2005. Generalized Steady-State Analysis of Multiphase Interleaved Boost Converter with Coupled Inductors. In: Proc. IEE Electronics Power Application. 152(3): 584-594.

[10] R. Seyezhai and B.L. Mathur. Design Consideration of Interleaved Boost Converter for Fuel Cell Systems. International Journal of Advanced Engineering Sciences and Technologies. 7(2): 323-329.

[11] Hwang J.J., Chang W.R., Weng F.B., Su A. and Chen C.K. 2008. Development of a small vehicular PEM fuel cell system. Int. Journal of Hydrogen Energy. 33: 3801-3807.

[12] R. Seyezhai and B.L. Mathur. 2011. Mathematical Modeling of Proton Exchange Membrane Fuel Cell. International Journal of Computer Applications. 20(5): 0975-8887.

[13] Spiegel C. 2008. PEM Fuel Cell Modeling and Simulation Using Matlab. Elsevier Inc.

[14] Larminie J. and Dicks A. 2001. Fuel Cell System Explained. John Wiley and Sons Ltd., Chichester.